J Mol Model (2016) 22: 123
DOI 10.1007/s00894-016-2998-9

ORIGINAL PAPER

Theoretical insight into the binding energy and detonation performance of ε-, γ-, β-CL-20 cocrystals with β-HMX, FOX-7, and DMF in different molar ratios, as well as electrostatic potential

Rui-zhi Feng[1] · **Shu-hai Zhang**[1] · **Fu-de Ren**[1] · **Rui-jun Gou**[1] · **Li Gao**[1]

Received: 6 February 2016 / Accepted: 24 April 2016 / Published online: 11 May 2016

Abstract Molecular dynamics method was employed to study the binding energies on the selected crystal planes of the ε-, γ-, β-conformation 2,4,6,8,10,12-hexanitrohexaazaisowurtzitane (ε-, γ-, β-CL-20) cocrystal explosives with 1,1-diamino-2,2-dinitroethylene (FOX-7), 1,3,5,7-tetranitro- 1,3,5,7-tetrazacyclooctane with β-conformation (β-HMX) and *N*,*N*-dimethylformamide (DMF) in different molar ratios. The oxygen balance, density, detonation velocity, detonation pressure, and surface electrostatic potential were analyzed. The results indicate that the binding energies E_b^* and stabilities are in the order of 1:1 > 2:1 > 3:1 > 5:1 > 8:1 (CL-20:FOX-7/β-HMX/DMF). The values of E_b^* and stabilities of the energetic-nonenergetic CL-20/DMF cocrystals are far larger than those of the energetic-energetic CL-20/FOX-7 and CL-20/β-HMX, and those of CL-20/β-HMX are the smallest. For CL-20/FOX-7 and CL-20/β-HMX, the largest E_b^* appears in the cocrystals with the 1:1, 1:2 or 1:3 molar ratio, and the stabilities of the cocrystals with the excess ratio of CL-20 are weaker than those in the cocrystals with the excess ratio of FOX-7 or β-HMX. In CL-20/FOX-7, CL-20 prefers adopting the γ-form, and ε-CL-20 is the preference in CL-20/β-HMX, and ε-CL-20 and β-CL-20 can be found in CL-20/DMF. The CL-20/FOX-7 and CL-20/β-HMX cocrystals with low molar ratios can meet the requirements of low sensitive high energetic materials. Surface electrostatic potential reveals the nature of the sensitivity change upon the cocrystal formation.

Keywords Binding energy · Cocrystal · Detonation performance · Electrostatic potential · Molar ratio · Molecular dynamics

Introduction

Power and safety are both the most concern in the field of energetic materials, but there is an essential contradiction between them: the highly energetic materials are often not safe, and at present the rareness of pure low-sensitive and highly energetic explosive has been found [1–8]. Due to the stringent requirements for both the low sensitivity and high power simultaneously, the cocrystallization of explosive, a technique by which a multicomponent crystal of several neutral explosive molecules forms in a defined ratio through non-covalent interactions (e.g., H-bond, electrostatic interaction, etc.) [9, 10], has attracted great interest since it can alleviate to a certain extent the power-safety contradiction [11–14]. Recently a lot of cocrystal explosives have been synthesized and characterized [14–29]. An evaluation of the power and safety of energetic cocrystals has been carried out [30]. The intermolecular interactions in energetic cocrystals have also been discussed [31].

The stability (sensitivity) and detonation performance (energy, detonation velocity, and detonation pressure, etc.) of cocrystal explosive could be influenced by the molar ratio of molecular combination. Generally, when a cocrystal has too much content of high energy explosive, the packing density and detonation performance will be increased with the possible increased explosive sensitivity. On the contrary, the sensitivity will be decreased in a cocrystal explosive with much content of the low energetic or non-energetic explosive, accompanied by the possible decreased packing density, energy, and detonation velocity. The high sensitivity, low density, and

✉ Rui-zhi Feng
fengruizhi1@hotmail.com

[1] School of Chemical and Environmental Engineering, North University of China, Taiyuan 030051, China

inferior detonation performance are all the disapproving properties of the energetic materials. The search for the stable insensitive and highly energetic explosive is the primary goal in the field of energetic material chemistry [1, 7, 13]. Therefore, the molar ratios of two or more kinds of explosive components should be controlled in a reasonable scope, and it is very necessary to clarify the influence of the ratio of molecular combination on the stability and detonation performance of cocrystal explosives, such as packing density, oxygen balance, detonation velocity, and detonation pressure, etc.

In most previous literature, only the cocrystal explosives with defined molecular ratio were synthesized and characterized. Very recently, our group computed firstly the structures and binding energies on the selected crystal planes in the different molar ratios of 1,3,5,7-tetranitro-1,3,5,7-tetrazacyclooctane (HMX)/nitroguanidine (NQ) [32], 2,4,6,8,10,12-hexanitrohexaazaisowurtzitane of ε-conformation (ε-CL-20)/NQ [33], and ε-CL-20/1,1-diamino-2,2-dinitroethylene (FOX-7) [34] cocrystals by molecular dynamics (MD) technology. The predicted results indicated that the cocrystals had the high forming probability in low molar ratio. To our knowledge, few theoretical investigations into the influences of molar ratios on the bonding and detonation performance of cocrystal explosives were presented.

The power of cocrystal explosive will be diluted [30]. To avoid too much power dilution in cocrystal explosives, very powerful coformers are favored. Thus, CL-20 was considered to be one of the most powerful applied coformers to design the cocrystal explosives. CL-20-based cocrystals of energetic-energetic materials were prepared, such as CL-20/2,4,6-trinitrotoluene (TNT) (in a 1:1 ratio) [13, 35], CL-20/HMX (in a 2:1 ratio) [14], and CL-20/benzotrifuroxan (BTF) (in a 1:1 ratio) [17]. Furthermore, CL-20 was also cocrystalized with some non-energetic compounds [19], such as CL-20/*N*,*N*-dimethylformamide (DMF) (in a 1:2 ratio), CL-20/1,4-dioxane (in a 1:4 ratio), etc. Although the energies in the energetic-nonenergetic cocrystals with CL-20 were diluted badly, they had shorter intermolecular distance and higher stability than the energetic-energetic CL-20 cocrystal explosives [31].

Under ambient temperature and pressure conditions, there are four crystalline forms of CL-20 (α, β, γ, ε) [36, 37], in which the ε-CL-20 form has the highest density and greatest stability [38]. However, up to now, no ε-form is observed in the cocrystal of CL-20, and the β- and γ-forms are favorable in the CL-20 cocrystals. For example, in the CL-20/BTF [17] and CL-20/TNT [13, 35] cocrystals, the CL-20 molecule adopts the β-form, and in CL-20/HMX, the β and γ-forms are both found [14]. In general, the morphology of a single crystal is affected by its lattice symmetry and the relative strength of the intermolecular interactions between molecules along different crystallographic directions [39], and the molecular interactions at the binder interfaces between two or more coformers of cocrystal depend on the types of crystal faces [32–34, 39]. These facts suggest that it is possible to clarify the reason for the formation of the different CL-20 morphology in cocrystal by using the comparison of the relative strength of the attachment energies or binding energies on the different crystal faces of different CL-20 morphology. The attachment energy or binding energy, which gives a useful prediction of the morphology [40] and controls the habit in various cocrystal growth models [34, 41], is defined as the energy released when an additional growth face of thickness d_{hkl} is attached to the crystal plane [42]. In general, the faces with more negative attachment energies or binding energies have stronger attractive interactions between two coformers of cocrystal. The stronger the attachment energy or binding energy on the cocrystal face of certain CL-20 morphology, the more stable this cocrystal is. With this in mind, very necessary in the energetic cocrystal material field is the investigation for the relative strength of binding energies between the coformers of cocrystal on the different cocrystal faces of the different CL-20 morphology.

In this work, we systemically investigate the binding energies of the ε-, γ-, and β-CL-20 cocrystal explosives with FOX-7, β-HMX, and DMF on the different cocrystal faces in the different molar ratios by the MD method. The molecular structures of CL-20, HMX, FOX-7, and DMF are shown in Fig. 1. Since the α-CL-20 is often a hemihydrate, the cocrystal explosive with α-CL-20 is not considered. The oxygen balance (OB), density (d), detonation velocity (V_D), and detonation pressure (P_D) are estimated. The surface electrostatic potential was also analyzed. Our aim is mainly to explore the reason (or nature) of the formation of the different CL-20 morphology in cocrystal and clarify the influence of the ratio of molecular combination on the stability and detonation performance of cocrystal explosives of CL-20. These studies can provide some novel insight for the design of the CL-20 cocrystal explosive.

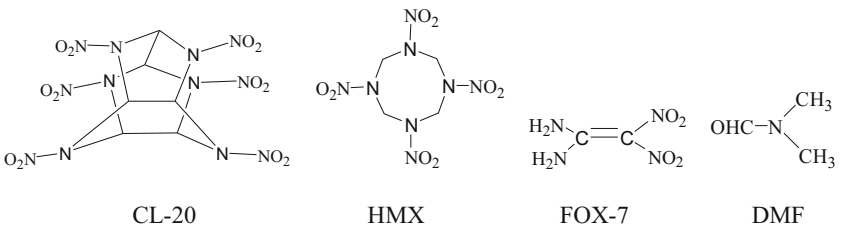

Fig. 1 Molecular structures of CL-20, HMX, FOX-7, and DMF

Computational details

Molecular dynamics calculations

The unit cell models of ε-, γ-, and β-CL-20 [43, 44], FOX-7 [45], and β-HMX [46, 47] were constructed according to their experimental cell parameters, respectively. Initial models were obtained by Discover module in COMPASS force-field; 1.0×10^{-5} kcal mol^{-1} of accuracy was required. The ε-, γ- and β-CL-20, FOX-7, and β-HMX crystal morphologies in vacuum were predicted by Growth morphology model.

Different cocrystal molar ratios can be treated by substituted method: molecules of ε-, γ- and β-CL-20 super cells were substituted by equal number of FOX-7, β-HMX or DMF at molar ratios of 8:1, 5:1, 3:1, 2:1, and 1:1 (CL-20:FOX-7/β-HMX/DMF). Molecules of FOX-7 or β-HMX super cells were substituted by equal number of CL-20 (ε-, γ- and β-forms) at molar ratios of 1:2, 1:3, 1:5, and 1:8 (CL-20:FOX-7 or β-HMX). Substituted molecules in this method were determined by the Miller indices *hkl*. The molar ratios, super cell patterns, and the number of substituted molecules are listed in Table 1.

For the substituted models, NVT ensembles were selected. Andersen was set as the temperature control method (298.15 K). COMPASS force-field was assigned. Summation methods for electrostatic and van der Waals were Ewald and Atom-based, respectively. The accuracy for Ewald method was 1.0×10^{-4} kcal mol^{-1}. Cutoff distance and buffer width for Atom-based method were 15.5 Å and 2.0 Å, respectively; 1.0 f. of time step was set for MD processes, and the total dynamic time was performed with 100,000 fs. All the MD calculations were carried out with MS 7.0 [48].

Because the binding energies of cocrystals obtained from the MD calculations are of different number of molecules, i.e., different super cells and different molecular molar ratios (see Table 1), and those of the same number of molecules should be adopted as a standard for assessing the component interaction strengths and stabilities of cocrystals. Therefore, according to our recent investigation [34], an energy correction formula for binding energy was used to standardize (uniform) the differences caused by diverse super cells and different molecular molar ratios as follows:

$$E_b^* = E_b \cdot N_0 \Big/ N_i \quad (1)$$

,where E_b^* denotes the binding energy after corrected, and N_i and N_0 are the number of molecules for different super cells and a standard pattern (molar ratio in 1:1), respectively. The binding energy E_b is calculated by the following formula:

$$E_b = E_{tot} - \left(nE_{CL-20} + mE_{FOX-7 \Big/ \beta\text{-}HMX \Big/ DMF} \right) \quad (2)$$

,where E_{tot}, $E_{CL\text{-}20}$ or $E_{FOX\text{-}7/\beta\text{-}HMX/DMF}$ is single point energy of cocrystal or monomer; n and m are the number of monomers in cocrystal.

Quantum-chemical calculations

The CL-20:FOX-7 (1:1) and CL-20:HMX (1:1) complexes with the intermolecular C−H···O−NO hydrogen bonds as well as the CL-20:DMF (1:1) complexes with the intermolecular C−H···O=C contacts were selected and optimized at the B3LYP/6-311++G** level. The most stable structures corresponding to the minimum energy points at the molecular energy hypersurface (NImag=0) were obtained. The above calculations were performed with Gaussian 09 [49]. The electrostatic potentials on the 0.001 au molecular surface are computed by the Multiwfn programs [50], utilizing the B3LYP/6-311++G** optimized geometries.

Detonation performance calculations

Except for HMX/FOX-7(1:1) [34], CL-20/β-HMX (2:1) [14], and CL-20/DMF (1:2) cocrystals [19], the experimental densities of cocrystals in this work can not be obtained since they

Table 1 The molar ratios, super cell patterns, and the number of substituted molecules

Molar ratio [a]	Super cell	Total number of molecules	Number of substituted molecules
8:1	3×3×2	72	8
5:1	3×2×2	48	8
3:1	2×2×2	32	8
2:1	3×2×2	48	16
1:1	2×2×2	32	16
1:2	3×2×2	48	16
1:3	2×2×2	32	8
1:5	3×2×2	48	8
1:8	3×3×2	72	8

[a] For the ratios of 8:1, 5:1, 3:1, 2:1, and 1:1, molar ratio means CL-20:FOX-7, CL-20:β-HMX or CL-20:DMF. For the ratios of 1:2, 1:3, 1:5, and 1:8, molar ratio means CL-20:FOX-7 and CL-20:β-HMX

have not been synthesized. However, Zhang *et al*. have found that there is a good linear relationship between the theoretical mixing density (d_{mix}) and experimental cocrystal density at room temperature (d_{298K}) [30]. Thus, the d_{298K} can be predicted through the d_{298K}–d_{mix} relationship. Here, we calculated the d_{mix} using Eq. (3) and supposed that the systems were composed of mixtures of pure components,

$$d_{mix} = \frac{\Sigma m_i}{\Sigma m_i \Big/ d_{298K,i}} \tag{3}$$

where m_i is the mass of component *i*. $d_{298K,i}$ is the density of component *i* at room temperature.

According to the literature [30], the density of cocrystal at room temperature (d_{298K}) is calculated by Eq. (4).

$$d_{298K} = 0.9967 d_{mix} \pm 0.005 \tag{4}$$

For a cocrystal with a formula of $C_aH_bO_cN_d$, its OB is computed by Eq. (5).

$$OB = \frac{c - 2a - b/2}{c} \times 100\% \tag{5}$$

According to the literature [30], V_D of cocrystal is calculated by Eq. (6).

$$V_D = 9.5863 + 0.0155OB + \left(1.7218 \times 10^{-5}\right)OB^2 + \left(7.0106 \times 10^{-9}\right)OB^3 \tag{6}$$

,where V_D is in km/s, and OB is in %.

Based on the above MD simulation of substituted models, the lattice energy was calculated. The heat of formation of a solid cocrystal (HOF(s)) is the summation of its lattice energy and the heats of formation of the gaseous state of molecules (HOF(g)). Since the HOF (g) values obtained from the semiempirical PM6 calculations are close to those computed by the DFT-B3LYP/6-31G* method [51], HOF(g) was calculated by using the PM6 method. The heats of detonation reactions (Q_D) were obtained by calculating HOF differences. V_D and P_D can be evaluated by Kamlet approximation, as shown by Eqs. (7) and (8) [52]:

$$V_D = 1.01\left(N^2\overline{M}Q_D\right)^{\frac{1}{4}}(1 + 1.30 d_{298K}) \tag{7}$$

$$P_D = 1.558\left(N^2\overline{M}Q_D\right)^{\frac{1}{2}} d_{298K}^2 \tag{8}$$

,where N is the moles of gaseous detonation products per gram of explosive and $\overline{M}$ is the average molecular weight of gaseous products. The design of detonation reactions proceeds according to the principle of the most heat release. Therefore, V_D was also evaluated by Kamlet approximation.

Results and discussion

Molecular dynamics analysis

There are seven major growth faces of isolated ε-CL-20 in vacuum: (0 1 1), (1 1 0), (1 0–1), (0 0 2), (1 1–1), (0 2 1), and (1 0 1). Their percentage areas are 34.00%, 21.79%, 16.71%, 9.44%, 6.86%, 6.71%, and 4.50%, respectively. There are six growth faces of isolated γ-CL-20 in vacuum: (1 0–1), (0 1 1), (1 0 1), (0 0 2), (1 1 0), and (1 1–1), among which (1 0–1), (0 1 1), and (1 0 1) are the main growth faces with percentage area of 34.65%, 25.00%, and 13.28%, respectively, and the percentage area of (0 0 2) or (1 1–1) is no more than 5.00%. Jessica *et al*. found that (0 0 1) and (0 1 0) were the main growth faces in actual β-CL-20 crystals [39]. Our calculated results indicate that the percentage areas of the (0 0 1) and (0 1 0) faces of β-CL-20 are 31.82% and 39.76%, respectively. Therefore, in this work, these growth faces and random face of ε-, γ- and β-CL-20 were selected to study the binding energies of the cocrystals with FOX-7, β-HMX, and DMF in different molar ratios, respectively.

Five major growth faces of FOX-7 were found: (0 1 1), (1 0 1), (1 0–1), (0 0 2), and (1 1–1). For β-HMX, there are also five major growth faces: (0 1 1), (1 1–1), (0 2 0), (1 0–2), and (1 0 0), among which (0 2 0) is the most stable. These growth faces and random face of FOX-7 and β-HMX were selected to study the binding energies of cocrystals.

CL-20/FOX-7 cocrystal

The binding energy E_b^* can supply a general evaluation for screening the preferable substituted pattern and molecular ratio. Based on the MD simulation of substituted models, E_b^* of the ε-, γ-, and β-CL-20 cocrystal explosives with FOX-7 on the different cocrystal faces in the different molar ratios are calculated (see Table 2).

From Table 2, E_b^* of cocrystallized ε-CL-20/FOX-7 patterns can be divided into two situations according to substituted models at molar ratios of 8:1, 5:1, 3:1, 2:1, 1:1 and 1:2, 1:3, 1:5, 1:8 (ε-CL-20:FOX-7). For the first situation, the binding energies E_b^* are in the order of 1:1 > 2:1 > 3:1 > 5:1 > 8:1, indicating that it is more stable for FOX-7 to replace CL-20 in the 1:1 molar ratio.

For the second situation, the binding energies E_b^* do not always decrease with the increasing mole ratio of FOX-7. For (0 1 1), (1 1 0), and (1 0 1), the binding energies E_b^* are in the order of 1:2 > 1:3 > 1:5 > 1:8. However, for (1 0–1), (1 1–1) and Random, they are in the order of 1:3 > 1:2 > 1:5 > 1:8, i.e., they reach a maximum at a molar ratio of 1:3.

Table 2 The corrected binding energy (in kJ mol mol^{-1}) of the substituted models of CL-20/FOX-7

		8:1	5:1	3:1	2:1	1:1	1:2	1:3	1:5	1:8
ε [a]	(0 1 1)	−337.2	−625.4	−972.3	−1204.2	−1165.2	−1262.8	−1224.7	−844.1	−607.2
	(1 1 0)	−303.0	−578.6	−748.5	−1125.2	−1383.6	−1417.7	−1232.2	−1115.3	−642.2
	(1 0–1)	−348.2	−619.5	−807.7	−1125.9		−1183.1	−1189.3	−806.4	−677.0
	(0 0 2)	−323.2	−523.8	−839.4	−946.4	−1136.5	−1206.7	−787.9	−728.4	−761.1
	(1 1–1)	−365.2	−490.0	−867.1	−1079.2	−1290.4	−1074.0	−1267.2	−911.7	−624.6
	(0 2 1)	−372.5	−572.9	−964.2	−1031.1	−1368.5				
	(1 0 1)	−416.6	−523.0	−938.2	−1184.7	−1422.7	−1122.6	−927.9	−871.6	−681.2
	Random	−381.5	−581.4	−946.3	−1097.3	−1589.0	−1361.4	−1446.0	−1078.0	−822.1
γ	(0 1 1)	−393.6	−503.1	−918.0	−1023.5	−1231.6	−1288.0	−1140.1	−1028.2	−518.3
	(1 1 0)	−363.5	−511.2	−940.2	−1101.6	−1456.7	−1605.1	−1387.0	−1179.4	−735.1
	(1 0–1)	−452.6	−543.1	−815.2	−1128.4	−1489.2	−1588.2	−1311.8	−1056.6	−726.0
	(0 0 2)	−428.3	−511.6	−762.3	−878.5	−1003.9	−1257.3	−1157.3	−967.8	−732.3
	(1 1–1)	−420.3	−493.1	−659.3	−815.2	−979.2	−1137.0	−1024.5	−922.3	−657.1
	(0 2 1)	−466.0	−526.3	−762.1	−912.1	−1218.1				
	(1 0 1)	−431.8	−527.6	−988.6	−1215.1	−1345.5	−1322.1	−1252.3	−977.8	−511.6
	Random	−378.9	−515.8	−927.5	−1288.4	−1587.2	−1369.7	−1201.5	−835.6	−417.5
β	(0 0 1)	−367.0	−578.9	−913.4	−1007.5	−1137.6				
	(0 1 0)	−389.1	−618.0	−985.6	−1123.7	−1165.2				
	Random	−408.5	−579.3	−866.2	−1252.8	−1443.6	−1532.7	−1276.8	−828.1	−497.6

[a] Data from ref. [34]

Furthermore, when compared to the binding energies E_b^* in 1:2 and 1:3, the values in 1:1 are not always the largest, indicating that the ε-CL-20/FOX-7 cocrystal in the 1:1 molar ratio is not always the most stable. The binding energy has been used as a scale factor indicating how the molecule is strongly attached to the crystal face [53]. Thus, the majority of FOX-7 molecules would cocrystallize with CL-20 molecules in the most stable substituted pattern, which has the strongest binding energy (or attachment energy). On (0 1 1), (1 1 0), and (0 0 2) facets, the binding energies E_b^* in 1:2 are larger than those in 1:1, showing that the ε-CL-20/FOX-7 cocrystal with the 1:2 molar ratio may be easier to be synthesized in these cocrystal faces. On (0 1–1), the binding energy E_b^* in 1:3 is close to that in 1:1, suggesting that the ε-CL-20:FOX-7 (1:3) cocrystal is also synthesized. In the other cocrystal faces, the binding energies E_b^* in 1:1 are the strongest, indicating that the ε-CL-20:FOX-7 (1:1) cocrystals are the preference.

Moreover, in the low ratios of 1:1 and 1:2, the binding energies E_b^* on random and (1 1 0) are the strongest. Therefore, the ε-CL-20/FOX-7 cocrystals on the random and (1 1 0) faces are the most stable, and the cocrystallization of ε-CL-20/FOX-7 are dominated by these two facets. As mentioned above, the percentage area of (0 1 1) is the largest, while the binding energies E_b^* on it is not the strongest. This is perhaps because the area percentage of the (0 1 1) face of ε-CL-20 was changed due to the intermolecular interaction between ε-CL-20 and FOX-7. The previous investigation has indicated that the area percentage of the cocrystal face can be changed. For example, Shen *et al.* found that the area percentage of the (0 1 1) face of β-CL-20 was increased up to 12.51 % in p-xylene solution from 7.81 % in vacuum due to the strong solvent interaction [54].

Table 2 also shows the binding energies E_b^* of cocrystallized γ-CL-20/FOX-7 patterns on the different crystal planes at molar ratios of 8:1, 5:1, 3:1, 2:1, 1:1 and 1:2, 1:3, 1:5, 1:8. For all the cocrystal faces, the order of the binding energy and stability is 1:1 > 2:1 > 3:1 > 5:1 > 8:1. For the cocrystals with the excess ratio of FOX-7, in the (1 0 1) and random, the order is 1:1 > 1:2 > 1:3 > 1:5 > 1:8, while in (0 1 1), (1 1 0), and (1 0–1), the order is 1:2 > 1:1 > 1:3 > 1:5 > 1:8, and for (0 0 2) and (1 1–1), that is 1:2 > 1:3 > 1:1 > 1:5 > 1:8. For the (1 0 1) and random, the binding energy and stability in 1:1 are the strongest, while for the other cocrystal faces, those in 1:2 are the strongest.

From Table 2, in the low ratios of 1:1 and 1:2, the binding energies E_b^* on random, (1 1 0), (1 0–1), and (1 0 1) are stronger than those in the other faces. Therefore, the γ-CL-20/FOX-7 cocrystals in these cocrystal facets are the most stable, and the cocrystallization of γ-CL-20/FOX-7 are dominated by them. In the 1:2 ratio, the binding energies E_b^* on (1 0–1) and (1 1 0) are larger than those on the other facets. As mentioned above, the percentage area of (1 0–1) is the largest. Furthermore, the oxygen atoms are observed exposed on it. The (1 0 1) face is rather open and rough on the molecular level with nitro groups, hydrogen, and oxygen atoms of the CL-20 exposed on the surface. Thus, γ-CL-20 can

cocrystallize with FOX-7 by the N–H···O and C–H···O intermolecular hydrogen bonds, and strong H-bonding can be formed between them. This is also probably one of the reasons that γ-CL-20/FOX-7 prefers cocrystalizing on (1 0–1) and (1 0 1). On the contrary, the (0 0 2) face is smooth on the molecular level, suggesting that it is difficult for FOX-7 to cocrystallize with γ-CL-20. Therefore, the binding energy E_b^* on it is weak.

For the (0 0 1), (0 1 0), and random faces of the β-CL-20/FOX-7 cocrystals with the excess ratio of β-CL-20, the order of the binding energy and stability is 1:1 > 2:1 > 3:1 > 5:1 > 8:1 (see Table 2). For the cocrystals with the excess ratio of FOX-7, the order is 1:2 > 1:1 > 1:3 > 1:5 > 1:8 on random. For (0 0 1) and (0 1 0), the binding energy and stability in 1:1 are the strongest, while for the random cocrystal faces, those in 1:2 are the strongest.

In the low ratios of 1:1 and 2:1, the binding energies E_b^* are in the order of random > (0 1 0) > (0 0 1), while in the ratios of 3:1, 5:1, and 8:1, E_b^* follows the order of (0 1 0) > random > (0 0 1). Except for random in 1:1, for each of the ratios, the binding energies E_b^* among three cocrystal faces are very close, no more than 250.0 kJ mol mol^{-1} of a difference among them.

As can be seen from Table 2, except for random, there is a trend that the strongest binding energies E_b^* in the γ-CL-20/FOX-7 are larger than those in ε-CL-20/FOX-7 and β-CL-20/FOX-7. Furthermore, for γ-CL-20/FOX-7, the binding energies E_b^* on the (1 1 0) and (1 0–1) cocrystal faces of FOX-7 in 1:2 and those on the (1 0–1) and (1 1 0) faces of γ-CL-20 in 1:1 are larger than the other cases. These results indicate that FOX-7 may prefer cocrystalizing with γ-CL-20 on the (1 1 0) and (1 0–1) faces of FOX-7 in 1:2, or on the (1 0–1) and (1 1 0) faces of γ-CL-20 in 1:1. It is noted that, as mentioned above, for the cocrystal with the excess ratio of FOX-7, the FOX-7 super cells were substituted by equal number of CL-20, while in the cocrystal with the excess ratio of CL-20, the CL-20 super cells were substituted by FOX-7.

CL-20/β-HMX cocrystal

For ε-CL-20/β-HMX, except for the random situation in the 1:3 ratio, the binding energies E_b^* are in the order of 1:1 > 2:1 > 3:1 > 5:1 > 8:1 and 1:2 > 1:3 > 1:5 > 1:8 (see Table 3). For random, the order is 1:3 > 1:2 > 1:5 > 1:8, i.e., the binding energy reaches a maximum at the molar ratio of 1:3. These results indicate that it is more stable for β-HMX to replace ε-CL-20 in the 1:1, 1:2, and 1:3 molar ratios.

Similar to ε-CL-20/FOX-7, when compared to the binding energies E_b^* in 1:2 and 1:3, the values in 1:1 are also not always the largest, indicating that the ε-CL-20/β-HMX cocrystal in 1:1 is not always the most stable. On (0 1 1), (1 1–1), and (0 2 0), the binding energies E_b^* in 1:2 are larger than those in 1:1, showing that the ε-CL-20/β-HMX cocrystal with the 1:2 molar ratio may be more stable on these three faces. On random, the binding energy in 1:1 is less than that in 1:3. On the other cocrystal faces, the binding energies E_b^* in 1:1 are the strongest, indicating that the ε-CL-20:β-HMX (1:1) cocrystals are more stable.

Table 3 The corrected binding energy (in kJ mol^{-1}mol) of the substituted models of CL-20/β-HMX

		8:1	5:1	3:1	2:1	1:1	1:2	1:3	1:5	1:8
ε	(0 1 1)	−287.3	−411.5	−618.0	−813.7	−928.3	−1105.2	−912.6	−680.5	−527.3
	(1 1–1)	−304.8	−423.7	−635.8	−891.5	−1057.5	−1089.7	−868.3	−715.9	−518.0
	(1 1 0)	−326.7	−503.2	−628.0	−855.3	−996.7				
	(1 0–1)	−287.1	−562.3	−723.5	−837.0	−938.2				
	(1 0 1)	−332.0	−640.5	−798.1	−917.2	−1068.9				
	(0 2 0)					−1105.1	−1187.9	−956.3	−723.8	−511.9
	Random	−303.4	−417.6	−625.7	−815.2	−989.6	−914.8	−1025.2	−801.6	−615.3
γ	(0 1 1)	−317.9	−415.5	−725.8	−846.4	−1006.8	−1015.2	−988.7	−769.9	−382.5
	(1 1–1)	−339.6	−427.8	−529.6	−702.6	−828.0	−1056.9	−1001.2	−618.9	−529.6
	(1 1 0)	−288.0	−379.9	−630.8	−792.5	−968.3				
	(1 0–1)	−375.0	−504.8	−723.6	−889.3	−1003.7				
	(1 0 1)	−315.4	−468.7	−670.1	−808.3	−987.1				
	(0 2 0)					−1037.9	−984.3	−912.0	−685.7	−443.0
	Random	−322.6	−487.0	−701.1	−889.5	−967.5	−1017.2	−814.7	−640.2	−355.9
β	(0 0 1)	−388.5	−518.3	−727.6	−915.1	−1026.5				
	(0 1 0)	−367.0	−479.5	−658.3	−921.4	−1000.8				
	(0 2 0)					−819.1	−826.2	−719.3	−552.8	−476.8
	Random	−336.9	−415.2	−703.6	−845.4	−975.1	−1013.5	−836.7	−613.5	−427.6

From Table 3, in 1:1 and 1:2, the binding energies E_b^* on (0 1 1), (1 1–1), (1 0 1), and (0 2 0) are stronger than those on (1 1 0), (1 0–1), and random. Therefore, the ε-CL-20/β-HMX cocrystals on (0 1 1), (1 1–1), (1 0 1), and (0 2 0) are more stable, and the cocrystallization of ε-CL-20/β-HMX are dominated by these four facets.

For the γ-CL-20/β-HMX cocrystal, the order of the binding energy and stability is 1:1 > 2:1 > 3:1 > 5:1 > 8:1. For all the cocrystals with the excess ratio of β-HMX, the order of the binding energy and stability follows 1:2 > 1:3 > 1:5 > 1:8. Except for random, for each of the cocrystal faces, the binding energies in 1:2 and 1:3 are very close to each other. For (0 2 0), the binding energy in 1:1 is larger than that in 1:2. However, for (0 1 1) and random, the binding energies in 1:1 are less than those in 1:2, and on (1 1–1), the binding energy in 1:1 is even less than that in 1:2 or 1:3.

From Table 3, for the γ-CL-20/β-HMX cocrystal, in the low ratios of 1:1 and 1:2, the binding energies E_b^* on (0 1 1), (1 1–1), and (0 2 0) are the strongest. Therefore, the γ-CL-20/β-HMX cocrystals on the (0 1 1), (1 1–1), and (0 2 0) faces are the most stable, and the cocrystallization of ε-CL-20/β-HMX are dominated by these three facets. It should be mentioned that, in the ratios of 1:1 and 1:2, the binding energies in all the cocrystal faces are close, with the largest difference of 158.9 kJ mol^{-1}. These results show that, although γ-CL-20 prefers cocrystalizing with β-HMX on the (0 1 1), (1 1–1), and (0 2 0) faces, the cocrystallization on the other faces, such as (1 1 0), (1 0–1), and (1 0 1), could also form.

From Table 3, for the β-CL-20/β-HMX, the order of the binding energy and stability is 1:1 > 2:1 > 3:1 > 5:1 > 8:1 for (0 0 1), (0 1 0), and random cocrystal faces. For the cocrystals with the excess ratio of β-HMX, the order is 1:2 > 1:1 > 1:3 > 1:5 > 1:8. For (0 0 1) and (0 1 0), the binding energy and stability in 1:1 are the strongest, while for the (0 2 0) and random cocrystal faces, those in 1:2 are the strongest.

In the ratios of 1:1 and 2:1, the binding energies E_b^* on (0 1 0) and (0 0 1) are larger than that on (0 2 0). Furthermore, the binding energies E_b^* on (0 1 0) and (0 0 1) are very close to each other. These results suggest that β-CL-20 prefers cocrystalizing with β-HMX on the (0 1 0) and (0 0 1) faces.

As can be found from Table 3, the strongest binding energies E_b^* in the ε-CL-20/β-HMX are larger than those in γ-CL-20/β-HMX and β-CL-20/β-HMX.

Furthermore, for ε-CL-20/β-HMX, the binding energies E_b^* on the (0 2 0) and (0 1 1) cocrystal faces of β-HMX in 1:2 and 1:1 are larger than the other cases. These results indicate that β-HMX prefers cocrystalizing with ε-CL-20 on (0 2 0) and (0 1 1) in 1:2 or 1:1. However, it is not the case: ε-CL-20/β-HMX is not synthesized but the γ-CL-20/β-HMX and β-CL-20/β-HMX cocrystals have been found [14]. Furthermore, from Table 3, the binding energies in the cocrystals with the excess ratio of β-HMX are far larger than those in the cocrystals with the excess ratio of CL-20, suggesting the cocrystals with the excess ratio of β-HMX are more stable than the cocrystals with the excess ratio of CL-20, and the former should be synthesized more easily than the latter. However, a 2:1 cocrystal of CL-20:HMX was reported by experiment [14], while the 1:2 cocrystal of CL-20:HMX was not synthesized. It should be emphasized that the factors influencing the formation of cocrystallization are complicated: besides the binding energy, some more important factors like the solvent effect and temperature effect should also be considered.

As can also be found from Table 3, the strongest binding energies E_b^* in γ-CL-20/β-HMX are close to those in β-CL-20/β-HMX, suggesting these two kinds of cocrystals may coexist. Indeed, Bolton *et al.* found that both the β- and γ-forms of CL-20 occupied half in the CL-20:HMX (2:1) cocrystals [14].

CL-20/DMF cocrystal

High energy is one of requirements of energetic materials, and the detonation performance (such as detonation velocity and detonation pressure) of the cocrystal with the excess ratio of the high energetic CL-20 may be better than that with the excess ratio of DMF. Since DMF is a nonenergetic molecule, the energy will be decreased in the cocrystal with the excess ratio of DMF. Therefore, in the energetic material field, the cocrystal with the excess ratio of CL-20 is more important

Table 4 The corrected binding energy (in kJ mol^{-1}) of the substituted models of CL-20/DMF

		8:1	5:1	3:1	2:1	1:1
ε	(0 1 1)	−528.9	−1369.5	−1982.0	−2285.2	−2318.5
	(1 1 0)	−467.5	−1527.0	−2160.3	−2537.9	−2606.3
	(1 0–1)	−511.8	−1428.8	−2189.1	−2415.3	−2582.9
	(0 0 2)	−546.0	−1348.0	−1884.0	−2188.5	−2389.3
	(1 1–1)	−689.3	−1425.6	−2202.5	−2468.7	−2687.2
	(0 2 1)	−712.0	−1566.7	−1879.3	−2132.3	−2218.6
	(1 0 1)	−456.8	−1460.1	−2137.6	−2418.6	−2689.0
	Random	−478.0	−1357.9	−2219.0	−2461.7	−2517.8
γ	(0 1 1)	−468.9	−1392.8	−1769.7	−1998.3	−2167.3
	(1 1 0)	−721.0	−1476.0	−1992.5	−2013.5	−2259.3
	(1 0–1)	−493.1	−1502.8	−2209.6	−2459.7	−2602.8
	(0 0 2)	−475.6	−1437.0	−1755.8	−1987.9	−2147.5
	(1 1–1)	−491.7	−1388.5	−1629.0	−1979.0	−2015.8
	(0 2 1)	−524.8	−1416.9	−1781.8	−1852.6	−2189.7
	(1 0 1)	−477.6	−1512.6	−1832.7	−2127.9	−2318.0
	Random	−428.5	−1378.0	−1902.6	−2218.6	−2454.6
β	(0 0 1)	−459.1	−1568.7	−2235.8	−2409.3	−2628.7
	(0 1 0)	−427.3	−1479.8	−2167.9	−2380.1	−2579.3
	Random	−462.9	−1523.9	−2083.7	−2357.0	−2589.0

Table 5 Predicted properties at different molar ratios

	OB(%)	d_{mix} (g/cm)	d_{298K} (g/cm)	V_D (km/s)	N (mol/g)	$\overline{M}$ (g mol^{-1})	Q_D (kcal/kg)	$V_{D(K-J)}$ (km/s)	P_D (GPa)
γ-CL-20	−25.000		1.916 [a]				1305.87 [a]	9.12 [a]	38.8 [a]
64γ-CL-20:8FOX-7	−26.000	1.915	1.908	9.195	0.034502	28.98	1300.05	9.0968	38.715
40γ-CL-20:8FOX-7	−26.563	1.914	1.908	9.187	0.034645	28.86	1296.77	9.1004	38.746
24γ-CL-20:8FOX-7	−27.500	1.913	1.906	9.173	0.034884	28.67	1291.32	9.1003	38.722
32γ-CL-20:16FOX-7	−28.571	1.911	1.905	9.157	0.035156	28.44	1285.09	9.1029	38.732
16γ-CL-20:16FOX-7	−31.250	1.908	1.901	9.119	0.035836	27.90	1269.57	9.1052	38.705
16γ-CL-20:32FOX-7	−35.000	1.903	1.896	9.065	0.036785	27.19	1247.90	9.1092	38.681
8γ-CL-20:24FOX-7	−37.500	1.899	1.893	9.029	0.037415	26.73	1233.51	9.1111	38.661
8γ-CL-20:40FOX-7	−40.625	1.895	1.889	8.985	0.038200	26.18	1215.57	9.1112	38.615
8γ-CL-20:64FOX-7	−43.182	1.892	1.886	8.949	0.038841	25.75	1200.94	9.1114	38.581
FOX-7	−50.000		1.883 [b]				1167.86 [c]	8.93 [d]	28.4 [c]
ε-CL-20	−25.000		2.044 [e]				1294.95 [a]	9.53 [f]	43.3 [a]
64ε-CL-20:8β-HMX	−26.923	2.032	2.026	9.181	0.034737	28.79	1282.53	9.4821	43.509
40ε-CL-20:8β-HMX	−27.941	2.026	2.020	9.167	0.034996	28.57	1275.96	9.4666	43.296
24ε-CL-20:8β-HMX	−29.545	2.017	2.010	9.143	0.035404	28.25	1265.62	9.4416	42.949
32ε-CL-20:16β-HMX	−31.250	2.007	2.000	9.119	0.035836	27.90	1254.66	9.4149	42.589
16ε-CL-20:16β-HMX	−35.000	1.985	1.979	9.065	0.036785	27.19	1230.62	9.3602	41.849
16ε-CL-20:32β-HMX	−39.286	1.961	1.955	9.004	0.037864	26.41	1203.27	9.2930	40.967
8ε-CL-20:24β-HMX	−41.667	1.949	1.942	8.970	0.038462	26.00	1188.13	9.2556	40.486
8ε-CL-20:40β-HMX	−44.231	1.935	1.928	8.934	0.039103	25.57	1171.87	9.2138	39.956
8ε-CL-20:64β-HMX	−46.053	1.925	1.919	8.908	0.039558	25.28	1160.34	9.1873	39.620
β-HMX	−50.000		1.905 [f]				1135.44 [a]	9.000 [f]	38.3 [a]

[a] The data comes from ref. [30]

[b] The data comes from ref. [45]

[c] The data comes from ref. [55]

[d] The data comes from ref. [56]

[e] The data comes from ref. [43]

[f] The data comes from ref. [57]

than that with the excess ratio of DMF. So in this work, only the excess ratio of CL-20 was discussed.

The binding energies E_b^* are summarized in Table 4. For the ε-, γ-, and β-CL-20/DMF cocrystal on all the faces, the values of E_b^* in the ratios of 1:1, 2:1, and 3:1 are close to each other, and the largest difference between 1:1 and 3:1 is 552.0 kJ mol^{-1}, and the maximum deviation of E_b^* between the ratios of 1:1 and 3:1, defined as $[(E_b^*{}_{(max)} - E_b^*{}_{(min)})/E_b^*{}_{(min)})] \times 100\%$, is 22.49%. This result shows that the stabilities of the cocrystals in the ratios of 1:1, 2:1, and 3:1 are very close. Since the γ-CL-20/DMF cocrystal in 1:1 has been synthesized [19], the cocrystals of the 2:1 and 3:1 ratios can also be synthesized by the suitable method.

The differences of binding energies between 3:1 and 5:1 are large (up to about 700.0 kJ mol^{-1}), showing that, from 3:1 to 5:1, the binding energies and stabilities of cocrystals decrease remarkably. The differences of binding energies between 5:1 and 8:1 are larger, in the range of 700.0~1000.0 kJ mol^{-1}. The deviations of E_b^* between the ratios of 5:1 and 8:1, defined as $[(E_b^*{}_{(max)} - E_b^*{}_{(min)})/E_b^*{}_{(min)})] \times 100\%$, are in the range of 50.0~80.0%.

For all of the substituted patterns, the binding energies E_b^* are in the same order of 1:1 > 2:1 > 3:1 > 5:1 > 8:1. In the ratios of 1:1, 2:1, and 3:1, the binding energies are the largest, and thus CL-20/DMF cocrystal may prefer cocrystalizing in the 1:1, 2:1, and 3:1 molar ratios. In other words, the cocrystal in the low ratio might be stable. In deed, most of the energetic-nonenergetic cocrystal explosives with the 1:1 or 2:1 molar ratio are reported experimentally [19].

From Table 4, in the ratio of 1:1, for the ε-CL-20/DMF cocrystals, the binding energies E_b^* on (1 0 1), (1 1–1), (1 1 0), and (1 0–1) are stronger than those in the other cocrystal faces. Therefore, the ε-CL-20/DMF cocrystals on (1 0 1), (1 1–1), (1 1 0), and (1 0–1) are more stable, and the cocrystallizations of ε-CL-20/DMF are dominated by these four facets. For the γ-CL-20/DMF cocrystals, the binding

energy in (1 0–1) is far stronger than those on the other cocrystal faces. For the β-CL-20/DMF cocrystals, the binding energies in three cocrystal faces ((0 0 1), (0 1 0), and random) are close. Therefore, the γ-CL-20 and β-CL-20 cocrystals with DMF are dominated by the (1 0–1), (0 0 1), and (0 1 0) facets, respectively. As a whole, the binding energies in the γ-CL-20/DMF cocrystals are weaker than those in the ε-CL-20/DMF and β-CL-20/DMF cocrystals, suggesting that DMF prefers cocrystalizing with ε-CL-20 and β-CL-20, and the stabilities of ε-CL-20/DMF or β-CL-20/DMF cocrystal are higher than those of γ-CL-20/DMF.

All in all, from Tables 2, 3, and 4, for all the cocrystals, the binding energies E_b^* and stabilities are in the same order of 1:1 > 2:1 > 3:1 > 5:1 > 8:1, suggesting that the cocrystals with the low ratios are synthesized more easily. Moreover, the values of E_b^* of the CL-20/DMF cocrystals in all the substituted patterns with all the ratios are far larger than the corresponding results of the CL-20/FOX-7 or CL-20/β-HMX cocrystals, suggesting that the energetic-nonenergetic CL-20/DMF might be cocrystallized more easily than the energetic-energetic cocrystals CL-20/FOX-7 and CL-20/β-HMX. This is perhaps due to the strong electron donating C=O group in DMF which can form strong intermolecular H-bonds with the C–H group of CL-20.

From Tables 2 and 3, the binding energies E_b^* in 1:1 are not always the largest, and the largest E_b^* may also appear in the cocrystals with the 1:2 or 1:3 molar ratio. This result shows that the cocrystals in 1:1 are not always the most stable, and it is more stable for CL-20 to replace FOX-7 or β-HMX in the 1:2 and 1:3 molar ratios. Furthermore, the values of E_b^* of CL-20/FOX-7 are larger than the corresponding results of CL-20/β-HMX, indicating that CL-20/FOX-7 might be cocrystallized more easily than the CL-20/β-HMX. For CL-20/FOX-7 and CL-20/β-HMX cocrystals, the binding energies E_b^* in the cocrystals with the excess ratio of CL-20 are weaker than those in the cocrystals with the excess ratio of FOX-7 or CL-20/β-HMX, suggesting that the stabilities in the former are weaker than those of the latter.

By the comparison of the relative strength of the binding energies on the different crystal faces of the different CL-20 morphology, we can draw a conclusion as follows: β-HMX prefers cocrystalizing with ε-CL-20 on the (0 2 0) and (0 1 1) cocrystal faces of β-HMX in the ratio of 1:2 or 1:1; FOX-7 may prefer cocrystalizing with γ-CL-20 on the (1 1 0) and (1 0–1) cocrystal faces of FOX-7 in the ratio of 1:2, or on the (1 0–1) and (1 1 0) cocrystal faces of γ-CL-20 in the ratio of 1:1. The stabilities of ε-CL-20/DMF and β-CL-20/DMF cocrystal are higher than those of γ-CL-20/DMF. In other words, in the CL-20/FOX-7 cocrystal, the CL-20 molecule prefers adopting the γ-form, and ε-CL-20 is the preference in the CL-20/β-HMX cocrystal. ε-CL-20 and β-CL-20 can be found in the CL-20/DMF cocrystal.

Density, oxygen balance, detonation velocity, and detonation pressure

The density (d), oxygen balance (OB), detonation velocity (V_D), detonation pressure (P_D), and heats of detonation reactions (Q_D) have been adopted to evaluate the power of an explosive. In general, higher d, V_D, P_D, Q_D, and an OB closer to zero suggest higher power. OB has also been used as one of the indicators for safety, as a more negative OB corresponds to higher safety. As mentioned above, in the CL-20/FOX-7 cocrystal, the CL-20 molecule prefers adopting the γ-form, while ε-CL-20 is the preference in the CL-20/β-HMX cocrystal. Therefore, OB, V_D, P_D, Q_D, and d of the energetic-energetic cocrystallized systems γ-CL-20/FOX-7 and ε-CL-20/β-HMX in the molar ratios 8:1, 5:1, 3:1, 2:1,

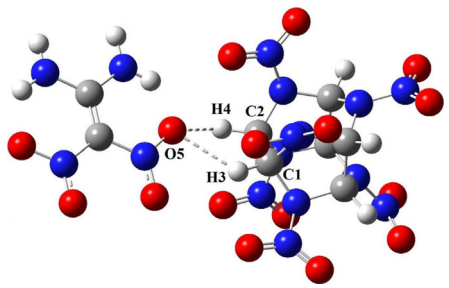

$R_{H4\cdots O5}$=2.524 Å $R_{H3\cdots O7}$=2.857 Å

CL-20···FOX-7

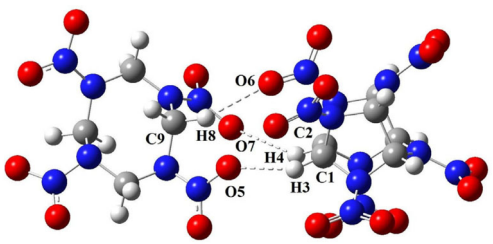

$R_{H4\cdots O7}$=2.502 Å $R_{H3\cdots O5}$=2.918 Å $R_{H8\cdots O6}$=3.117 Å

CL-20···HMX

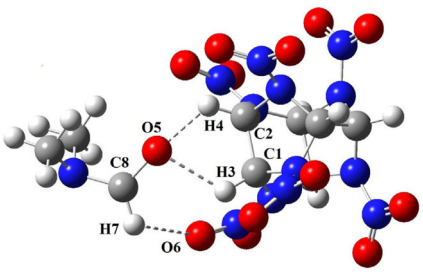

$R_{H3\cdots O5}$=2.305 Å $R_{H4\cdots O5}$=2.419 Å $R_{H7\cdots O6}$=3.280 Å

CL-20···DMF

Fig. 2 The optimized geometries (the most stable structures) of CL-20···FOX-7, CL-20···HMX and CL-20···DMF at the B3LYP/6-311++G** level

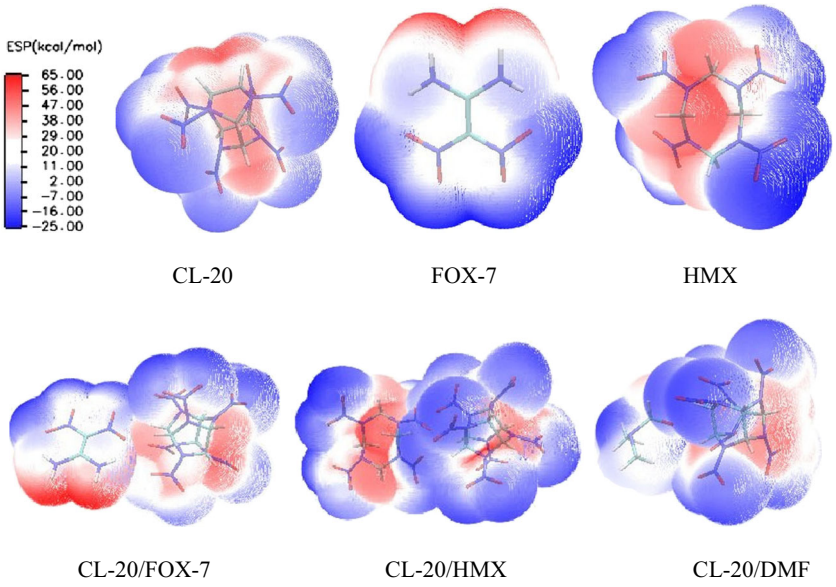

Fig. 3 Surface electrostatic potentials of monomers and complexes

1:1 and 1:2, 1:3, 1:5, 1:8 (CL-20:FOX-7/HMX) are calculated (see Table 5).

From Table 5, for γ-CL-20/FOX-7, with the increases of the components of FOX-7, the values of V_D predicted through the V_D–OB relationship are decreased, while those computed by using the Kamlet-Jacobs equations are almost unchanged, close to 9.1 km/s. For ε-CL-20/β-HMX, although the values of V_D obtained from the V_D–OB relationship are smaller than those from the Kamlet-Jacobs equations (in each of the molar ratios, the difference between them is about 0.3 km/s), the values computed by using two methods have the same variation tendency: with the increases of the components of β-HMX, the values of V_D are decreased.

On one hand, for γ-CL-20/FOX-7 and ε-CL-20/β-HMX, the OB values become more negative after cocrystallization in contrast to that of the pure CL-20, leading to a possible lower sensitivity than CL-20. On the other hand, the values of d, V_D, P_D, and Q_D are compromised by two related components, indicating that the power of CL-20 is diluted by FOX-7 or HMX. Moreover, the more the component of FOX-7 or HMX is, the more notable the dilution of CL-20 power becomes.

However, d, V_D, P_D, and Q_D of CL-20/FOX-7 and CL-20/HMX cocrystals in the molar ratios of 3:1, 2:1, 1:1 and 1:2, 1:3 are not too much different with the pure CL-20. For example, the P_D values of CL-20/FOX-7 are about 38.7 GPa, very close to 38.8 GPa of the pure CL-20. In other words, the power of CL-20 is not diluted badly in these molar ratios. Therefore, the cocrystals in the molar ratios of 3:1, 2:1, 1:1 and 1:2, 1:3 are satisfactory in view of explosive properties, and they can meet the requirements of the low sensitive high energetic materials. Combining with the results of binding energies (binding energies in 1:1 to 1:3 or 1:1 to 3:1 are very close), the investigation into the cocrystals with the ratios of 3:1, 2:1, 1:1 and 1:2, 1:3 will be meaningful for experimental research.

Structure and surface electrostatic potential of the CL-20 complex (1:1) with FOX-7, HMX, and DMF

In order to get more information on the bonding and stability of cocrystals, the most stable complexes (1:1) of CL-20 with FOX-7, HMX and DMF are investigated at the B3LYP/6-311++G** level (see Fig. 2). The intermolecular H-bonds between the hydrogen atom of the C–H bond of CL-20 and

Table 6 Molecular surface electrostatic potentials (in kcal mol^{-1}), positive and negative variances (σ_+^2, and σ_-^2 (in (kcal $mol^{-1})^2$)) as well as electrostatic balance parameter $\frac{\sigma_+^2\sigma_-^2}{(\sigma_+^2+\sigma_-^2)^2}$ (ν)

	CL-20	FOX-7	HMX	CL-20···FOX-7	CL-20···HMX	CL-20···DMF
$V_{s,min}$	−15.81	−33.36	−26.75	−29.85	−24.93	−22.21
$V_{s,max}$	67.75	62.55	62.51	65.96	65.28	50.28
$V_{s,max}$ (N/C–NO_2)	29.34 29.89	19.21	18.22	23.35(FOX-7)		28.30(CL-20)
σ_+^2	232.74	250.82	251.21	225.99	254.68	126.66
σ_-^2	16.46	77.21	43.97	45.15	28.89	24.85
ν	0.0617	0.1800	0.1268	0.1388	0.0915	0.1371

the oxygen atom of the NO_2 group in HMX are found, as is in accordance with the experimental results of the ε-CL-20/β-HMX cocrystal by the single crystal X-ray diffraction method [14]. The hydrogen bonds between the hydrogen atom of CL-20 and the oxygen atom in FOX-7 and DMF are also confirmed by the accepted O···H distances of H-bonds. Therefore, the CH hydrogen bonding can play an important role in stabilizing the cocrystals of CL-20 with FOX-7, HMX, and DMF. In the cocrystals of CL-20 with TNT [13] and BTF [17], the CH hydrogen bonding was also found.

Electrostatic potential (ESP) is a real and fundamentally significant physical property of compounds [58]. The surface electrostatic potential has been taken into account in the analysis of the sensitivity of the pure explosives [59–65] and cocrystal explosives, such as the CL-20/TNT [20] and HMX/FOX-7 cocrystal [32]. In order to reveal the nature of sensitivity change upon the formation of cocrystal, the surface electrostatic potentials of CL-20, HMX, FOX-7, and their cocrystals as well as the CL-20/DMF cocrystal are investigated. The results are shown in Fig. 3 and Table 6.

Politzer *et al*. have found that the local maximum above the C−NO_2 or N−NO_2 bond ($V_{S,max}$ (C/N−NO_2)) links to the impact sensitivity: the more positive the value of $V_{s,max}$ (C/N−NO_2), the higher the sensitivity becomes [63, 66–68]. From Table 6, for CL-20···FOX-7, the $V_{S,max}$ of the N−NO_2 bonds in CL-20 changes very slightly, while the $V_{S,max}$ of the C−NO_2 bonds in FOX-7 is increased from 19.21 kcal mol^{-1} in pure component to 23.35 kcal mol^{-1} in the complex, indicating that the C−NO_2 bonds become weak and the sensitivity of FOX-7 in the complex is increased in comparison with those in the pure FOX-7. In CL-20···HMX, the $V_{S,max}$ of the N−NO_2 bonds involving the H-bonds in CL-20 or HMX can not be distinguished from the strongly positive potential of hydrogen or N atoms of the −NO_2 group. In CL-20···DMF, the $V_{S,max}$ involving the N−NO_2 bonds of CL-20 in the complex is slightly less positive than that in the isolated CL-20, indicating that the N−NO_2 bonds become strong and the sensitivity of CL-20 in the complex is decreased in comparison with that in the pure CL-20.

According to Politzer *et al*. [69], for the nitramine explosive, the smaller the value of positive variance of $V_S(r)$ (σ_+^2) is, and simultaneously the larger the value of electrostatic balance parameter $\frac{\sigma_+^2\sigma_-^2}{\left(\sigma_+^2+\sigma_-^2\right)^2}$ (ν) is, the lower the impact sensitivity h_{50} becomes. The values of σ_+^2, σ_-^2, and ν are also collected in Table 6. For CL-20···FOX-7 and CL-20···HMX, the value of σ_+^2 is close to that of pure CL-20, FOX-7 or HMX, but the value of ν is larger than that of pure CL-20 while lower than that of pure FOX-7 or HMX. Therefore, the impact sensitivity h_{50} of CL-20···FOX-7 or CL-20···HMX is lower than that of CL-20 while higher than that of FOX-7 or HMX. In CL-20···DMF, the value of σ_+^2 is far lower than that of pure CL-20, and simultaneously the value of ν is far larger than that of pure CL-20, leading to the decreased impact sensitivity h_{50} in comparison with the pure CL-20. It should be emphasized that, in fact, the factors influencing the stability (or sensitivity) are complicated. In particular, recently Politzer *et al*. have pointed out that a high detonation heat release is generally accompanied by high sensitivity; accordingly, the heat release must be kept moderate [65, 70]. Therefore, the heat release should also be considered for cocrystal explosives.

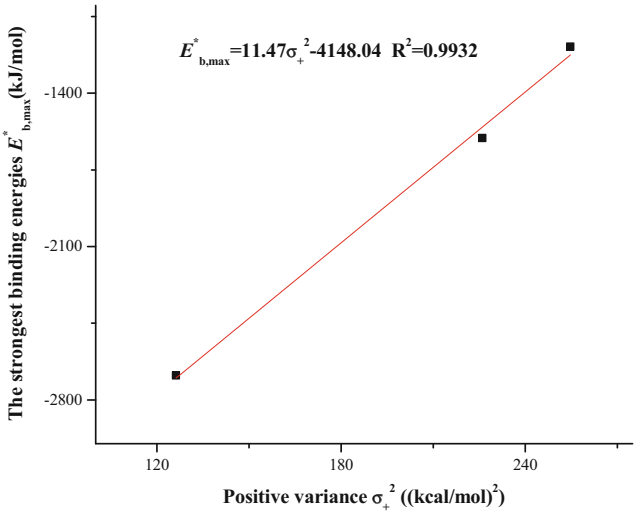

Fig. 4 Plot showing the strongest binding energies $E^*_{b,max}$ against positive variances σ_+^2

A good (R^2=0.9932) linear correlation is obtained between the strongest binding energies ($E^*_{b,max}$) and positive variances (σ_+^2) as shown in Fig. 4. They fit the following equation:

$$E^*_{b,max} = 11.47\sigma_+^2 - 4148.04 \quad (9)$$

This suggests that the electrostatic potentials are a good indicator of noncovalent interactions.

Conclusions

In this work, we systemically investigate the binding energies of the ε-, γ-, and β-CL-20 cocrystal explosives with FOX-7, β-HMX, and DMF on the different cocrystal faces in the different molar ratios by the MD method. The oxygen balance (OB), density (*d*), and detonation velocity (V_D) are estimated. The surface electrostatic potential was also analyzed. The results indicate that, for all the cocrystals, the binding energies E_b^* and stabilities are in the same order of 1:1 > 2:1 > 3:1 > 5:1 > 8:1, suggesting that the cocrystals with the low ratios are synthesized more easily. Moreover, the values of E_b^* of the CL-20/DMF cocrystals in all the substituted patterns with all the ratios are far larger than the corresponding results of the CL-20/FOX-7 and CL-20/β-HMX cocrystals, suggesting that the energetic-nonenergetic CL-20/DMF might be cocrystallized more easily than the energetic-energetic

cocrystals CL-20/FOX-7 and CL-20/β-HMX. For CL-20/FOX-7 and CL-20/β-HMX, the binding energies E_b^* in 1:1 are not always the largest, and the largest E_b^* may appear in the cocrystals with the 1:1, 1:2 or 1:3 molar ratio. Furthermore, the values of E_b^* of the CL-20/FOX-7 cocrystals are larger than the corresponding results of the CL-20/β-HMX cocrystals, indicating that CL-20/FOX-7 might be cocrystallized more easily than the CL-20/β-HMX. The binding energies E_b^* in the cocrystals with the excess ratio of CL-20 are weaker than those in the cocrystals with the excess ratio of FOX-7 or CL-20/β-HMX, suggesting that the stabilities in the former are weaker than those of the latter. β-HMX prefers cocrystalizing with ε-CL-20 on the (0 2 0) and (0 1 1) cocrystal faces of β-HMX in the ratio of 1:2 or 1:1. FOX-7 may prefer cocrystalizing with γ-CL-20 on the (1 1 0) and (1 0–1) cocrystal faces of FOX-7 in the ratio of 1:2, or on the (1 0–1) and (1 1 0) cocrystal faces of γ-CL-20 in the ratio of 1:1. DMF prefers cocrystalizing with ε-CL-20 and β-CL-20. In other words, in the CL-20/FOX-7 cocrystal, the CL-20 molecule prefers adopting the γ-form, and ε-CL-20 is the preference in the CL-20/β-HMX cocrystal. ε-CL-20 and β-CL-20 can be found in the CL-20/DMF cocrystal.

The CL-20/FOX-7 and CL-20/β-HMX cocrystal explosives with molar ratios of 1:1, 1:2, 1:3, 2:1, and 3:1 can meet the requirements of the low sensitive high energetic materials.

The surface electrostatic potential can be used to reveal the nature of the decreased sensitivity in complex (or cocrystal).

Acknowledgments This work was supported by Research for Shanxi Natural Science Foundation (2012021027–3) and Shanxi Provincial Projects for Science and Technology Development (20140311008–7).

Compliance with ethical standards

We have full control of all primary data and allow the journal to review all the data. We confirm the validity of the results. We have no financial relationships. The manuscript is not submitted to more than one journal, and it was not published previously. This study is not split up into several parts to increase the quantity of submissions. No data have been fabricated or manipulated.

References

1. Keshavarz MH, Pouretedal HR (2010) Simple relationship for predicting impact sensitivity of nitroaromatics, nitramines, and nitroaliphatics. Propellants Explos Pyrotech 35:175–181
2. Zhao J, Xu DH, Cheng XL (2010) Investigation of correlation between impact sensitivities and bond dissociation energies in some triazole energetic compounds. Struct Chem 21:1235–1240
3. Li JS (2010) A multivariate relationship for the impact sensitivities of energetic N-nitrocompounds based on bond dissociation energy. J Hazard Mater 174:728–733
4. Li JS (2010) A quantitative relationship for the shock sensitivities of energetic compounds based on X–NO_2 (X = C, N, O) bond dissociation energy. J Hazard Mater 180:768–772
5. Rice BM, Hare JJ (2002) A quantum mechanical investigation of the relation between impact sensitivity and the charge distribution in energetic molecules. J Phys Chem A 106:1770–1783
6. Tan BS, Long XP, Peng RF, Li HB, Jin B, Chu SJ, Dong HS (2010) Two important factors influencing shock sensitivity of nitro compounds: bond dissociation energy of X–NO_2 (X = C, N, O) and Mulliken charges of nitro group. J Hazard Mater 183:908–912
7. Delpuech A, Cherville J (1979) Relation entre la structure electronique et la sensibilité au choc des explosifs secondaires nitrés. Critère moléculaire de sensibilité II. Cas des esters nitriques. Propellants Explos Pyrotech 4:121–128
8. Xiao HM (1994) Molecular orbital theory of nitro-compound. Publishing House of Defense Industry, Peking
9. Jean-Marie L (1988) Supramolecular chemistry-scope and perspectives molecules, supermolecules, and molecular devices (Nobel Lecture). Angew Chem Int Ed 27:89–112
10. Lara-Ochoa F, Espinosa-Pérez G (2007) Cocrystals definitions. Supramol Chem 19:553–557
11. Kira BL, Onas B, Adam JM (2013) Two isostructural explosive cocrystals with significantly different thermodynamic stabilities. Angew Chem Int Ed 52:6468–6471
12. Zhang H, Guo C, Wang X, Xu J, He X, Liu Y, Liu X, Huang H, Sun J (2013) Five energetic cocrystals of BTF by intermolecular hydrogen bond and π-stacking interactions. Cryst Growth Des 13:679–687
13. Onas B, Matzger AJ (2011) Improved stability and smart-material functionality realized in an energetic cocrystal. Angew Chem Int Ed 50:8960–8963
14. Onas B, Simke LR, Pagoria PF, Matzger AJ (2012) High power explosive with good sensitivity: A 2:1 cocrystal of CL-20:HMX. Cryst Growth Des 12:4311–4314
15. Guo C, Zhang H, Wang X, Xua J, Liu Y, Liu X, Huang H, Sun J (2013) Crystal structure and explosive performance of a new CL-20/caprolactam cocrystal. J Mol Struct 1048:267–273
16. Wang Y, Yang Z, Li H, Zhou X, Zhang Q, Wang J, Liu Y (2014) A novel cocrystal explosive of HNIW with good comprehensive properties. Propellants Explos Pyrotech 39(4):590–596
17. Yang Z, Li H, Zhou X, Zhang C, Huang H, Li J, Nie F (2012) Characterization and properties of a novel energetic-energetic cocrystal explosive composed of HNIW and BTF. Cryst Growth Des 12:5155–5158
18. Evers J, Ivan G, Manuel J, Thomas MK, Jörg S (2014) Cocrystallization of photosensitive energetic copper(II) perchlorate complexes with the nitrogen-rich ligand 1,2-Di(1H-tetrazol-5-yl)ethane. Inorg Chem 53:11749–11756
19. David IAM, Helen EMC, David RA, Adam SC, Alistair RL, Alexandra JM, Iain DHO, Chiu CT, Colin RP (2012) Crystal engineering of energetic materials: Co-crystals of CL-20. CrystEngComm 14:3742–3749
20. Li H, Shu Y, Gao S, Chen L, Ma Q, Ju X (2013) Easy methods to study the smart energetic TNT/CL-20 co-crystal. J Mol Model 19: 4909–4917
21. Lin H, Zhu SG, Li HZ, Peng XH (2013) Synthesis, characterization, AIM and NBO analysis of HMX/DMI cocrystal explosive. J Mol Struct 1048:339–348
22. Wei C, Duan X, Liu C, Liu Y, Li J (2009) Molecular simulation on co-crystal structure of HMX/TATB. Acta Chim Sin 67:2822–2826
23. Jin PS, Duan XH, Luo QP, Zhou Y, Bao Q, Ma YJ, Pei CH (2011) Preparation and characterization of a novel cocrystal explosive. Cryst Growth Des 11:1759–1765
24. Wei C, Huang H, Duan X, Pei C (2011) Structures and properties prediction of HMX/TATB co-crystal. Propellants Explos Pyrotech 36:416–423

25. Landenberger KB, Matzger AJ (2012) Cocrystals of 1,3,5,7-Tetranitro-1,3,5,7-tetrazacyclooctane (HMX). Cryst Growth Des 12:3603–3609
26. Lin H, Zhu S, Li H, Peng X (2013) Structure and detonation performance of a novel HMX/LLM-105 cocrystal explosive. J Phys Org Chem 26:898–907
27. Lin H, Zhu S, Zhang L, Peng X, Chen P, Li H (2013) Intermolecular interactions, thermodynamic properties, crystal structure, and detonation performance of HMX/NTO cocrystal explosive. Int J Quantum Chem 113:1591–1599
28. Gu B, Lin H, Zhu S (2014) Ab initio studies of 1,3,5,7-tetranitro-1, 3,5,7-tetrazocine/ 1,3-dimethyl-2-imidazolidinone cocrystal under high pressure using dispersion corrected density functional theory. J Appl Phys 115:143509-1–143509-8
29. Lin H, Zhu SG, Zhang L, Peng XH, Li HZ (2014) Synthesis and first principles investigation of HMX/NMP cocrystal explosive. J Energ Mater 31:261–272
30. Zhang C, Cao Y, Li H, Zhou Y, Zhou J, Gao T, Zhang H, Yang Z, Jiang G (2013) Toward low-sensitive and high-energetic cocrystal I: evaluation of the power and the safety of observed energetic cocrystals. CrystEngComm 15:4003–4014
31. Zhang C, Xue X, Cao Y, Zhou J, Zhang A, Li H, Zhou Y, Xu R, Gao T (2014) Toward low-sensitive and high-energetic cocrystal II: structural, electronic and energetic features of CL-20 polymorphs and the observed CL-20-based energetic-energetic co-crystals. CrystEngComm 16:5905–5916
32. Li Y, Chen S, Ren F, Jin S (2015) Theoretical insights into the structures and mechanical properties of HMX/NQ cocrystal explosives and their complexes, and the influence of molecular ratios on their bonding energies. J Mol Model 21:245-1~245-13
33. Ding X, Gou R, Ren F, Liu F, Zhang S, Gao H (2015) Molecular dynamics simulation and density functional theory insight into the cocrystal explosive of hexaazaisowurtzitane/nitroguanidine. Int J Quantum Chem 2:88–96
34. Gao H, Zhang S, Ren F, Liu F, Gou R, Ding X (2015) Theoretical insight into the co-crystal explosive of 2,4,6,8,10,12-hexanitrohexaazaisowurtzitane (CL-20)/1,1-diamino-2,2-dinitroethylene (FOX-7). Comp Mater Sci 107:33–41
35. Yang Z, Li H, Huang H, Zhou X, Li J, Nie F (2013) Preparation and performance of a HNIW/TNT cocrystal explosive. Propellants Explos Pyrotech 38:495–501
36. Yan QL, Zeman S, Elbeih A, Song ZW, Málek J (2012) The effect of crystal structure on the thermal reactivity of CL-20 and its C4 bonded explosives (I): thermodynamic properties and decomposition kinetics. J Therm Anal Calorim 112:823–836
37. Bolotina NB, Hardie MJ, Speer RL Jr, Pinkerton A (2004) Energetic materials: variable-temperature crystal structures of Γ- and ε-HNIW polymorphs. J Appl Crystallogr 37:808–814
38. Holtz E, Ornellas D, Foltz MF, Clarkson JE (1994) The solubility of ε-CL-20 in selected materials. Propellants Explos Pyrotech 19:206–212
39. Jessica HU, Jennifer AS (2014) Solvent effects on the growth morphology and phase purity of CL-20. Cryst Growth Des 14:1642–1649
40. Beyer T, Day GM, Price SL (2001) The prediction, morphology, and mechanical properties of the polymorphs of paracetamol. J Am Chem Soc 123:5086–5094
41. Hartman P, Bennema P (1980) The attachment energy as a habit controlling factor: I. Theoretical considerations. J Cryst Growth 49: 145–156
42. Hartman P, Perdok WG (1955) On the relations between structure and morphology of crystals. I. Acta Cryst 8:49–52
43. Nielsen AT, Chafin AP, Christian SL, Moore DW, Nadler MP, Nissan RA, Vanderah DJ (1998) Synthesis of polyazapolycyclic caged polynitramines. Tetrahedron 54:11793–11812
44. Russell TP, Miller PJ, Piermarini GJ, Block S (1993) Pressure/ temperature phase diagram of hexanitrohexaazaisowurtzitane. J Phys Chem 97:1993–1997
45. Gilardi R (1999) CCCD 127539, Cambridge structural database. Cambridge Crystallographic Data Center, Cambridge
46. Chang BC, Choi S, Boutin HP (1970) A study of the crystal structure of β-cyclotetramethylene tetranitramine by neutron diffraction. Acta Crystallogr B 26:1235–1240
47. Choi CS, Prince H (1972) The crystal structure of cyclotrimethylenetrinitramine. Acta Crystallogr B 28:2857–2862
48. Accelrys Software Inc. (2013) Materials Studio 7.0. San Diego
49. Frisch MJ, Trucks GW, Schlegel HB, Scuseria GE, Robb MA, Cheeseman JR, Scalmani G, Barone V, Mennucci B, Petersson GA, Nakatsuji H, Caricato M, Li X, Hratchian HP, Izmaylov AF, Bloino J, Zheng G, Sonnenberg JL, Hada M, Ehara M, Toyota K, Fukuda R, Hasegawa J, Ishida M, Nakajima T, Honda Y, Kitao O, Nakai H, Vreven T, Montgomery JA, Jr, Peralta JE, Ogliaro F, Bearpark M, Heyd JJ, Brothers E, Kudin KN, Staroverov VN, Kobayashi R, Normand J, Raghavachari K, Rendell A, Burant JC, Iyengar SS, Tomasi J, Cossi M, Rega N, Millam JM, Klene M, Knox JE, Cross JB, Bakken V, Adamo C, Jaramillo J, Gomperts R, Stratmann RE, Yazyev O, Austin AJ, Cammi R, Pomelli C, Ochterski JW, Martin RL, Morokuma K, Zakrzewski VG, Voth GA, Salvador P, Dannenberg JJ, Dapprich S, Daniels AD, Farkas O, Foresman JB, Ortiz JV, Cioslowski J, Fox DJ (2009) Gaussian 09. Gaussian, Inc. , Wallingford
50. Lu T (2014) Multiwfn: a multifunctional wavefunction analyzer, version 3.3.5. Beijing
51. Stewart JJP (2007) Optimization of parameters for semiempirical methods V: modification of NDDO approximations and application to 70 elements. J Mol Model 13:1173–1213
52. Kamlet MJ, Jacobs SJ (1968) Chemistry of detonations. I. A simple method for calculating detonation properties of C–H–N–O explosives. J Chem Phys 48:23–35
53. Shim HM, Kim JW, Koo KK (2013) Molecular interaction of solvent with crystal surfaces in the crystallization of ammonium sulfate. J Cryst Growth 373:64–68
54. Shen F, Lv P, Sun C, Rubo Zhang R, Pang S (2014) The crystal structure and morphology of 2,4,6,8,10,12-hexanitro-2,4,6,8,10,12-hexaazaisowurtzitane (CL-20) *p*-Xylene solvate: a joint experimental and simulation study. Molecules 19:18574–18589
55. Trzciński WA, Cudziło S, Chyłek Z, Szymańczyk L (2008) Detonation properties of 1,1-diamino-2,2-dinitroethene (DADNE). J Hazard Mater 157:605–612
56. Latypov NV, Bergman J, Langlet A, Wellmar U, Bemm U (1998) Synthesis and reactions of 1,1-diamino-2,2-dinitroethylene. Tetrahedron 54:11525–11536
57. Dong H, Zhou F (1989) High energetic explosives and relatives. Beijing Science Press, Peking
58. Murray JS, Politzer P (2011) The electrostatic potential: an overview. WIREs Comput Mol Sci 1:153–163
59. Politzer P, Murray JS (2014) Impact sensitivity and crystal lattice compressibility/free space. J Mol Model 20:2223–2230
60. Murray JS, Concha MC, Politzer P (2009) Links between surface electrostatic potentials of energetic molecules, impact sensitivities and C–NO_2/N–NO_2 bond dissociation energies. Mol Phys 107:89–97
61. Politzer P, Murray JS (2014) In: Brinck T (ed) Green energetic materials. Wiley, Chichester, UK. doi:10.1002/9781118676448
62. Politzer P, Murray JS (2014) Detonation performance and sensitivity: a quest for balance. Adv Quantum Chem 69:1–30
63. Politzer P, Murray JS (1996) Relationships between dissociation energies and electrostatic potentials of C–NO_2 bonds: applications to impact sensitivities. J Mol Struct 376:419–424
64. Murray JS, Lane P, Politzer P (1998) Effects of strongly electron-attracting components on molecular surface electrostatic potentials:

application to predicting impact sensitivities of energetic molecules. Mol Phys 93:187–194

65. Politzer P, Murray JS (2015) Some molecular/crystalline factors that affect the sensitivities of energetic materials: molecular surface electrostatic potentials, lattice free space and maximum heat of detonation per unit volume. J Mol Model 21:25. doi: 10.1007/s00894-015-2578-4
66. Murray JS, Lane P, Politzer P (1995) Relationships between impact sensitivities and molecular surface electrostatic potentials of nitroaromatic and nitroheterocyclic molecules. Mol Phys 85:1–8
67. Politzer P, Murray JS (1995) C–NO_2 dissociation energies and surface electrostatic potential maxima in relation to the impact sensitivities of some nitroheterocyclic molecules. Mol Phys 86:251–255
68. Politzer P, Murray JS, Concha MC, Lane P (2007) Effects of electric fields upon energetic molecules: nitromethane and dimethylnitramine. Cent Eur J Energ Mater 4:3–21
69. Pospíšil M, Vávra P, Concha MC, Murray JS, Politzer P (2010) A possible crystal volume factor in the impact sensitivities of some energetic compounds. J Mol Model 16:895–901
70. Politzer P, Murray JS (2015) Impact sensitivity and the maximum heat of detonation. J Mol Model 21: 262.- doi: 10.1007/s00894-015-2793-z